Front. Earth Sci. 2020, 14(4): 828–841
https://doi.org/10.1007/s11707-020-0827-z

RESEARCH ARTICLE

Spatiotemporal variability of channel and bar morphodynamics in the Gorai-Madhumati River, Bangladesh using remote sensing and GIS techniques

Md. Yousuf GAZI (✉)[1], Farhad HOSSAIN[1], Sumiya SADEAK[1], Md. Mahin UDDIN[2]

1 Department of Geology, University of Dhaka, Dhaka-1000, Bangladesh
2 Department of Geography and Environment, University of Dhaka, Dhaka-1000, Bangladesh

Abstract Bangladesh is a riparian country that is criss-crossed by the many tributaries and distributaries of the mighty Ganges, Brahmaputra, and Meghna river systems. Gorai-Madhumati, a distributary of the Ganges River is an example where morphological development of the river is associated with frequent channel shifting within the catchment area. The main objective of this research is to quantify the extent of channel migration, erosion-accretion, river width, sinuosity, and charland morpho-dynamics from 1972 to 2018 using geospatial techniques combined with satellite images and hydrological data. The study also addressed the impacts of Farakka Barrage construction in India on the shifting, flow behavior, and siltation of Gorai-Madhumati River. The study shows that bar surface areas have abnormally increased in both segments after 1975 due to the construction of Farakka Barrage. Water flow in the Gorai-Madhumati has dropped remarkably in the downstream and instigated huge sedimentation in this region. Analysis of the time series satellite images revealed that the morphology of the river channel experienced huge changes simultaneously with the changes in the seasonal flow and sedimentation all over the study period. Migration trend has frequently shifted and taken place in the NW and NE direction in the observed sections of the river. Throughout the study period, total amount of accretion was greater than the net percentage of erosion on both banks of the river. River discharge, bar accretion, and erosion history show that the Gorai-Madhumati River will no longer exist with the present flowing condition without attention and proper river management.

Keywords channel migration, erosion-accretion, morphodynamics, geospatial techniques, Gorai-Madhumati, Bangladesh

Received February 11, 2020; accepted July 15, 2020

E-mail: yousuf.geo@du.ac.bd

1 Introduction

Bangladesh is a riparian basin that is traversed by numerous tributaries and distributaries of mighty Ganges, Brahmaputra, and Meghna river systems. River bank erosion and accretion with concurrent channel migration is a very common phenomenon and ongoing dynamic process in this country (Islam et al., 2014). River Bank shifting is often related to the event where one bank is forming and the opposite bank is eroding. Observing the spatiotemporal morphodynamics of a river is very crucial to comprehend the river behavior (Mondal et al., 2020). Bangladesh loses a plenty of fertile land and sandbanks every year due to riverbank erosion and flooding. Severe flood flows of the river water grind down the bank during the monsoon period whereas in the winter, sandbanks become deposited on the both banks of the river (Dabojani et al., 2014).

Gorai-Madhumati, a distributary of the Ganges River, is an example where morphological development of the river is associated with frequent channel shifting within the catchment area. Gorai-Madhumati holds a significant role in Bangladesh's river system in the southwestern part and is exposed to enormous changes due to natural and manmade causes (Hasan et al., 2015). Numerous studies have been initiated concerning the environment, hydrodynamics, ecosystems, morphological response, and bend development of the Gorai-Madhumati river system in Bangladesh (Clijncke, 2001; Islam and Karim, 2005; Islam and Gnauck, 2011; Hore et al., 2013; Biswas and Ahammad, 2014; Hasan et al., 2015; Khanam and Navera, 2016). Since the 1980s, the Gorai River flow has been choked by the deposition of sediment in the river course. After Farakka Barrage construction in India on the Ganges River in 1975, Ganges downstream water flow dropped remarkably. Farakka Barrage accelerated this process and influenced huge sedimentation in this region. With reduced

upstream water flow, vast amounts of sediments are transforming and depositing on the river channel. Consequently, morphology of the river is continuously changing (Khanam and Navera, 2016).

Riverine processes and morphological dynamics of river channels have been extensively studied by several researchers in the past 20 years (Surian, 1999; Winterbottom, 2000; Yang et al., 2002; Fuller et al., 2003; Rinaldi, 2003; Surian and Rinaldi, 2003; Li et al., 2007; Kummu et al., 2008; Ghoshal et al., 2010). Bag et al. (2019) studied channel geometry and migration of the Bhagirathi River in West Bengal, India. Remote sensing and GIS techniques are widely used for the quantification of erosion and deposition, and change detection of riverbanks worldwide. Several studies have assessed channel change by means of geospatial techniques, such as time series analysis of different satellite images (Downward et al., 1994; Marston et al., 1995; Gurnell, 1997; Dabojani et al., 2014; Bhuiyan et al., 2015; Magliulo et al., 2016; Langat et al., 2019) in diverse categories of river systems. Most of this research suggests that river dynamics are badly impacted by human intervention (different developmental activities and engineering construction). This human intervention results in remarkable channel change as process response (Das et al., 2012). This kind of changes in different parts of Bangladesh can be identified as a hazard. More significantly, it is a growing challenge for floodplain dwellers as it becoming more and more intensified in riverine basins of Bangladesh. The focal point of this study is to enumerate the extent of channel migration, calculate erosion-accretion from 1972 to 2018, and to investigate the impacts in the circumstances of riverine hazards. The present study also deals with the impacts of Farakka Barrage construction in India on the Gorai-Madhumati River shifting and siltation.

2 Study area

The Gorai-Madhumati River is one of the longest rivers in Bangladesh. In the upstream areas, it is named Gorai, and the name changes to Madhumati in the lower reaches (Ahmed and Islam, 2003). Gorai-Madhumati is a major right bank distributary of the Ganges River (Adams, 1919). The Gorai-Madhumati River catchment area is about 15160 km^2 with 199 km course length covering the part or full extent of Pabna, Chuadanga, Kushtia, Rajbari, Faridpur, Gopalgonj, Jessore, Jhenaidah, Magura, Norail, Pirojpur, Borguna, Bagerhat, Khulna, and Sathkhira districts of southwestern part of Bangladesh (Fig. 1) (Islam, 2003). The Gorai-Madhumati River discharges into the Bay of Bengal through the Passur River and Sibsa River. According to the 2011 population census (BBS, 2016), population of the catchment area is estimated at 15563000. The average annual rainfall varies between 2478 mm in the southeast and 1516 mm in the northeast. The mean temperature of the catchment area fluctuates between 23°C and 32°C in summer and 22°C to 23°C in the winter season (EGIS, 2000). It is considered as the prime source of fresh water for the part of Sundarbans mangrove wetlands and southwest region of Bangladesh (Islam and Gnauck, 2011). The bedload materials of the river vary from fine sand to silts in nature. The annual average transported sediment is around 50 million tons which includes 40% bedload materials and the remaining comprising of silt and clay (Halcrow et al., 1993; DHI, 1996). This area is divided into shallow depressions and valleys of mature deltaic river channels influenced by the monsoon climate which shaped long morphological changes in the reaches of the Gorai-Madhumati River. In the Gorai-Madhumati River system, flood discharge has recorded about 7000 m^3 in the monsoon phase but in the winter period, discharge goes down from 5 m^3 to almost 0 m^3 (Khanam and Navera, 2016). The Gorai-Madhumati River is 272.4 km far away from Farakka Barrage which was constructed in the upstream part of Ganges River in India.

3 Materials and methods

3.1 Overview

We combined satellite imagery (spanning 1972–2018), water discharge data (spanning 1970–2019), and statistical calculation to analyze the channel migration at an interval of 10 years by using GIS and RS techniques. Although selected satellite images have different spatial resolution, images were geometrically and radiometrically corrected before extracting bank lines. A precise digitization process has also been employed to compare the indices based extracted bank line. GIS technique is an effective and accurate tool of quantifying channel changes both at medium and short-term scales (Winterbottom, 2000). A number of Landsat (MSS, TM, ETM, OLI) imagery was acquired from the USGS Earth Explorer data hub and the images were selected using the daily water level data from 1970 to 2019 collected from the Bangladesh Water Development Board (BWDB) (Table 1). The fluctuation of water level and cloud cover was analyzed to select accurate satellite images. First of all, images were mosaicked through ERDAS IMAGINE 2014 and the study AOI was extracted from the images, then the modified normalized difference water index (*MNDWI*) was used to extract the bank line from the images. The channel planform characteristics such as width, sinuosity index, surface area of newly formed bars, and shifting of the right and left bank with direction of migration were calculated using ArcGIS 10.3 to quantify the channel migration (Fig. 2). Finally, the migration pattern and its possible causes and future trend was summarized on the basis of the changes in the channel trajectories.

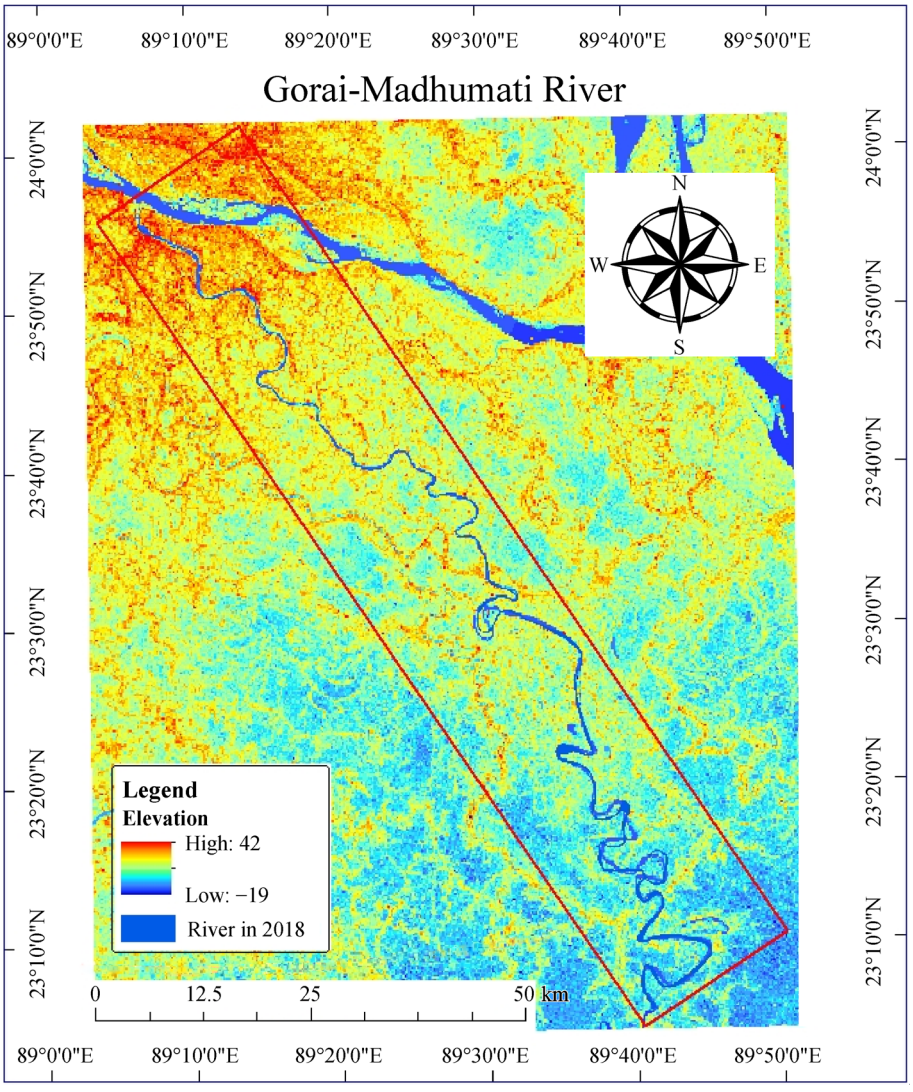

Fig. 1 The extent and course of the Gorai-Madhumati River in the southwestern part of Bangladesh (study area).

3.2 Satellite imagery selection based on water level data

To select accurate representative satellite imagery for river bank line extraction, concurrent stream water level data are the most important factor (Yang et al., 2015). To ensure the representative river bank line trajectory, the water level data from Gorai Railway Bridge gauging station spanning from 1970 to 2019 were analyzed (Fig. 3).

At an interval of 10 years (except 1972 and 1977) six satellite images of Landsat MSS, TM, ETM, and OLI sensors with minimum cloud cover were collected from the USGS Earth Explorer data hub (Table 1). The concurrent water level was in between 2.60 and 2.75 during the time of capturing these images which minimize the bank line shift effect due to variations in water level fluctuation (Fig. 3).

3.3 Bank Line Extraction using *NDWI* and *MNDWI*

The normalized difference water index (*NDWI*) was derived on a per pixel basis for the separation of water body from the background and extracting accurate bank line trajectories. The formula used for *NDWI* calculation was proposed by McFeeters (1996),

$$NDWI = \frac{\text{Green} - NIR}{\text{Green} + NIR}, \quad (1)$$

where Green and *NIR* represent the reflectance value in the green and near infrared bands respectively. Only for the Landsat MSS sensors images (1972, 1977, and 1980), *NDWI* was calculated due to lack of mid-infrared band.

The modified normalized difference water index (*MNDWI*) was calculated for Landsat TM, ETM, and

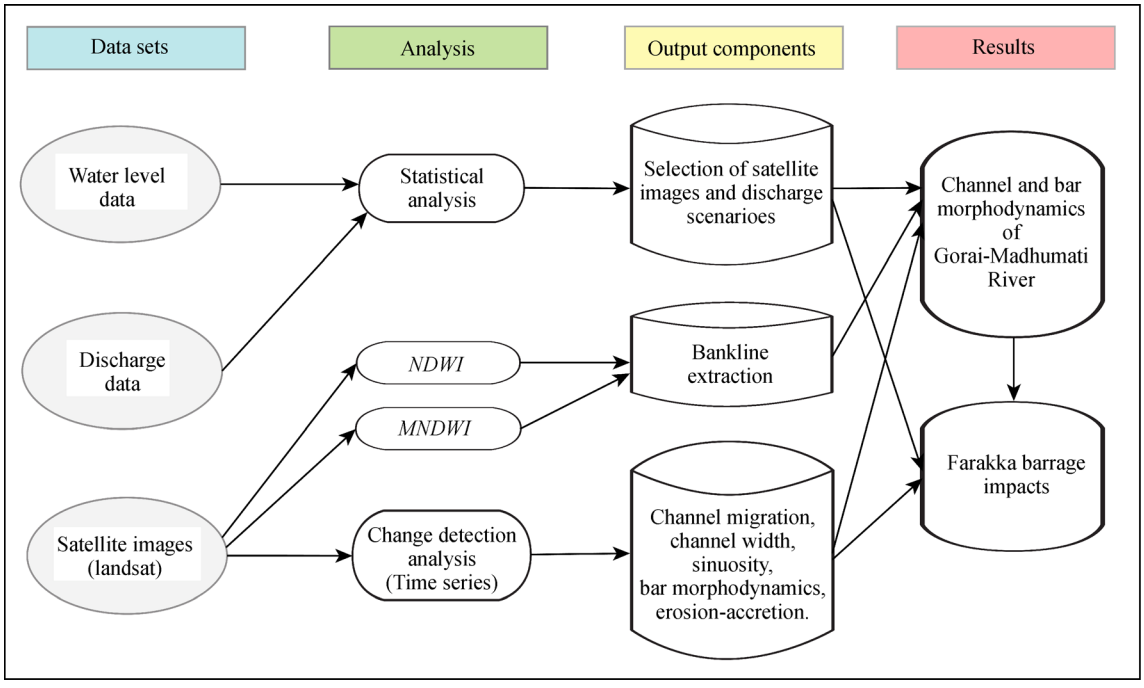

Fig. 2 The detail methodological workflow process undertaken in this study.

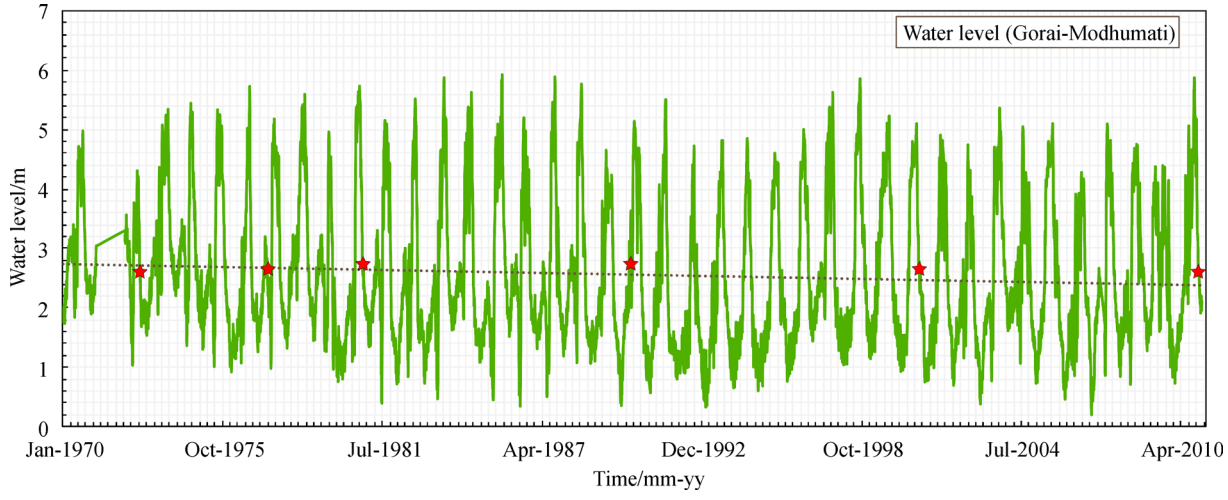

Fig. 3 Daily water level at the Gorai Railway Bridge station from 1970 to 2010 and the red star marks indicate respective water level during satellite image acquisition.

Table 1 Details of the acquired data set (satellite images, Discharge, water level and sediment load) used in the study

Year	Satellite images			Hydrological data		
	Sensor	Spatial resolution/m	Date of acquisition	Water level	Data	Source
1972	Landsat 1 MSS	60	18 Oct, 1972	2.702	Water level (Gorai Railway Bridge station)	BWDB
1977	Landsat 2 MSS	60	10 May, 1977	2.746		
1980	Landsat 3 MSS	60	29 Oct, 1980	2.743		
1990	Landsat 5 TM	30	16 Jun, 1990	2.789	Discharge (Hardringe Bridge Station)	
2000	Landsat 7 ETM	30	24 Oct, 2000	2.620		
2010	Landsat 5 TM	30	14 Nov, 2010	2.616		
2018	Landsat 8 OLI	30	30 Nov, 2019	–		

OLI images because these images have an MIR band. The formula for deriving *MNDWI* was proposed by Xu (2006),

$$MNDWI = \frac{\text{Green} - MIR}{\text{Green} + MIR}, \quad (2)$$

where Green and *MIR* represent the reflectance value in the green and mid-infrared bands respectively. *MNDWI* has a major advantage of reducing and even removing the built-up land noises over the *NDWI*.

The water body was extracted based on the optimum *NDWI* and *MNDWI* values. The boundary of the water body was considered as the bank line trajectory and the area inside the boundary represent the river channel and the existing sand bars. Vegetation and urbanized regions are found as negative values whereas water bodies including a river show values greater than zero.

3.4 Channel change detection and statistical analysis

The entire reach of the Gorai-Modhumati River was divided into 2 reaches: A and B. The migration of the river bank line over the study period is greater and well-visible in these reaches. Sinuosity, left and right bank shifting, net erosion and accretion, and sand bar dynamics were measured to depict the channel migration and morphodynamic processes. The direction of shifting, spatial variations in erosion and accretion, and location and surface area of sand bars were investigated to discuss the possible causes and future trends of bank line migration.

To calculate sinuosity index, the following equations are used based on (Fig. 4) (Morisawa, 1985).

$$\text{Sinuosity index} = (\text{Stream Length}) \times (\text{Valley Length})^{-1}, \quad (3)$$

$$\text{Sinuosity } (P) = XY \times (CD)^{-1}, \quad (4)$$

where *XY* is the length of the midline of the channel, *CD* is the overall length of the reach.

To calculate the river sinuosity index, the river (study area) was divided into two segments as A and B and the polygons were converted into polylines. The field geometry indicates the river length. The shortest length was calculated using the measure tool. The field calculator was used to calculate the sinuosity index.

4 Results and discussion

4.1 Spatiotemporal variation in river width

Seven satellite images (i.e., 1972, 1977, 1980, 1990, 2000, 2010, and 2018) have been studied to investigate morphological changes of the Gorai-Madhumati River utilizing morphometric techniques. To document the changes of width in the Gorai-Madhumati River, the study divided the river into two major segments, A and B, with segment B further divided into 12 sections (Fig. 5). From 1972 to 1977, major changes in river width pointed out in section 2 and section 5 where it was widened to about 198 m and 174 m consecutively, indicating erosion on both sides of the river bank. In contrast, the width of the river declined about the same amount (198 m) at section 3 between 1977 and 1980. Within this time frame, only segment A and sections 3, 7, 9, and 11 witnessed channels widening. In 1980–1990, the river width was highly reformed at section 3 and 1 where the width increased about 165 m and 111 m respectively (Table 2). However, section 5 showed a different scenario in which width decreased about 155 m. Minor variation in width occurred in section 4 and 10 representing 13 m and 8 m width dwindling, respectively.

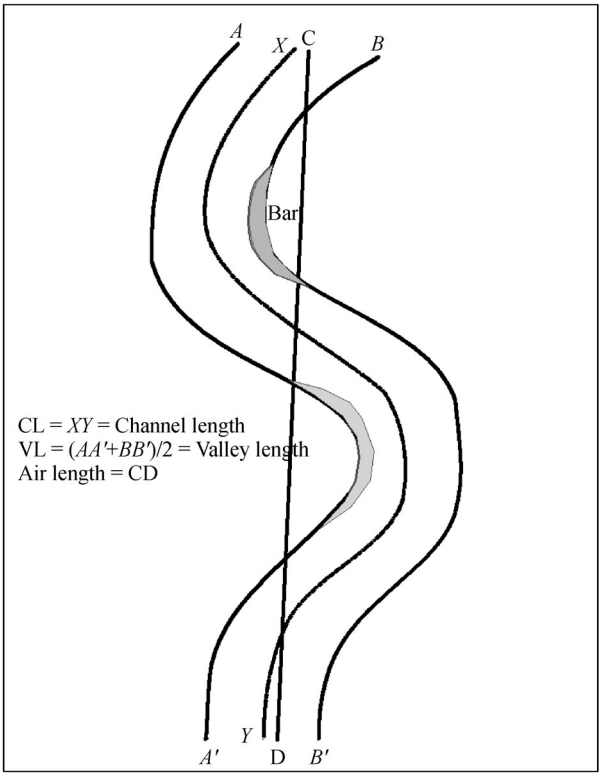

Fig. 4 The mathematical parameters of sinuosity calculation in a schematic diagram.

From 2000 to 2010, average width change was about 35 m in almost all river sections. The highest 98 m increased width was found in section 3, whereas only 1 m decreased width was observed in section 7. In the recent decade (2010–2018), almost all sections have shown that river width declined rapidly throughout this time frame except section 10 (Fig. 6). It is clear that the width decreased significantly at segment A which is about 286 m and the highest width change during the study period of 1972 to 2018. It is the evident that the Gorai-Madhumati channel is narrowing gradually from 1972 to 2018 throughout the

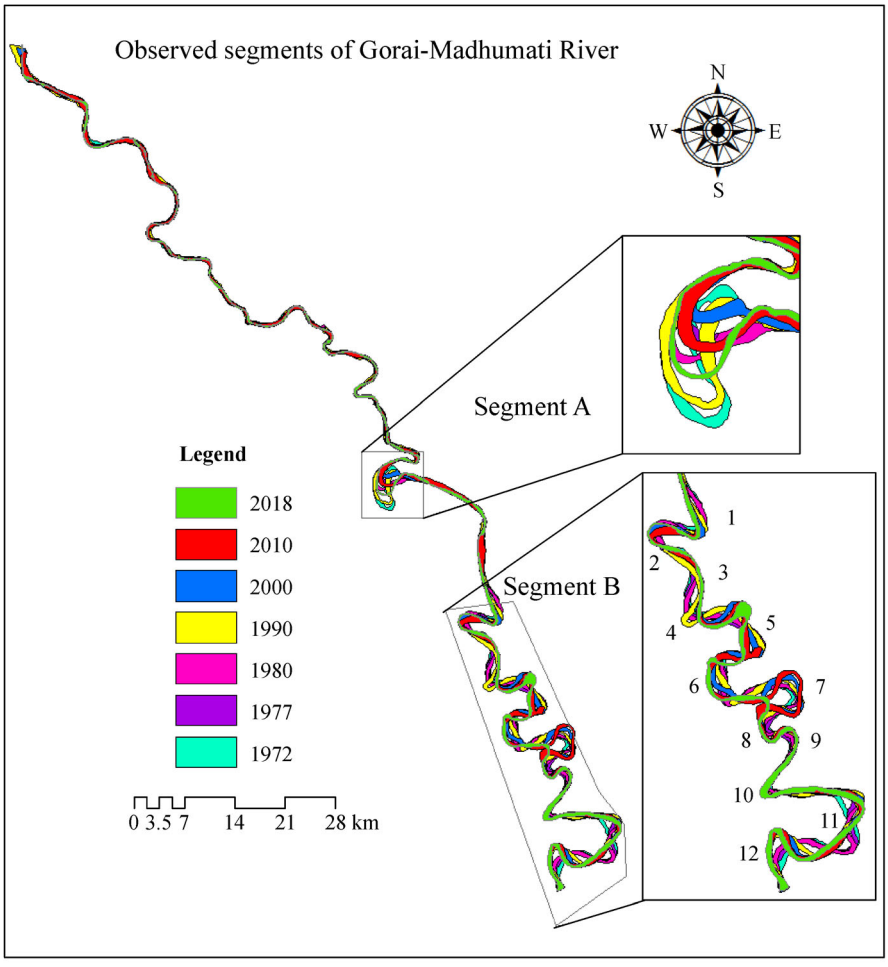

Fig. 5 Observed sections in the upstream, midstream and downstream part of the Gorai-Madhumati River from 1972 to 2018. Sections chosen based on the intensity and dynamism of natural riverine processes in the study area. Segment B further subdivided into 12 sections.

four decades and is becoming narrower at the current time. During the study period, average increased river width has noticed 118 m and the decreased width is about 82 m (Table 2). Many reasons are responsible for the resultant decreased river width. River morphology, decreasing the annual discharge, sedimentation process, and flow condition are key factors in this case. In Gorai-Madhumati, restricted flow in the river channel facilitated the deposition of sediments and simultaneously decreased the river width and depth which is similar to the outputs of some studies in different areas in Bengal Basin (Bhuiyan et al., 2015; Islam, 2016). Dams constructed are another obstacle that has interrupted the normal flow of the river (Islam, 2016).

4.2 Spatiotemporal lateral shifting of the river banks

Migration of left and right banks of the river channel in seven different years, i.e., 1972, 1977, 1980, 1990, 2000, 2010, and 2018 are documented in (Table 3). Gorai-Madhumati River shifted laterally in different directions with varied distance in the selected segments within the river floodplain (Fig. 7). Migration of the channel was accompanied by the alternating erosion in one bank and accretion in another bank. The result shows that erosion was prominent in the right bank from 1972 to 1977 in segment A. Maximum shifting observed in segment A which is about 3529 m from 1972 to 1977, 1088 m from 1977 to 1980, 2300 m from 1980 to 1990, 3261 m from 1990 to 2000, 1067 m from 2000 to 2010, and 1052 m from 2010 to 2018 for the right bank compared to the other segments. Now the channel is shifting from the NW to SE direction in segment A (Fig. 7). Among the 12 sections from segment B, right bank shifting was prominent in all sections except in 6 and 11 from 1972 to 1977. On the other hand, leftward channel movement was most evident from 1977 to 1980 in all sections except 1, 3, 4, 9, and 12.

From 1980 to 1990, maximum rightward and leftward

Table 2 Gorai River's sectional width changing pattern from 1972 to 2018. (+) value signifies channel widening and (−) value indicates the channel narrowing

Observed sections		Channel width changing pattern								
		Channel width 1972 /m	Channel width 1977 /m	Diff.	Channel width 1977 /m	Channel width 1980 /m	Diff.	Channel width 1980 /m	Channel width 1990 /m	Diff.
Segment A		563.40	465.70	−97.7	465.70	487.578	21.878	487.578	528.351	40.773
Segment B	1	338.46	348.105	9.645	348.105	333.439	−14.666	333.439	445.321	111.882
	2	404.584	603.146	198.562	603.146	405.083	−198.063	405.083	482.050	76.967
	3	396.908	368.054	−28.854	368.054	397.409	29.355	397.409	563.023	165.614
	4	469.150	439.568	−29.582	439.568	430.347	−9.221	430.347	416.867	−13.48
	5	411.104	586.034	174.93	586.034	582.305	−3.729	582.305	426.394	−155.911
	6	471.396	489.959	18.563	489.959	464.984	−24.975	464.984	517.260	52.276
	7	335.656	275.650	−60.006	275.650	324.631	48.981	324.631	295.598	−29.033
	8	323.408	412.328	88.92	412.328	317.409	−94.919	317.409	403.172	85.763
	9	307.864	331.339	23.475	331.339	353.096	21.757	353.096	335.099	−17.997
	10	323.480	366.354	42.874	366.354	361.647	−4.707	361.647	353.189	−8.458
	11	405.467	438.092	32.625	438.092	443.63	5.538	443.63	485.758	42.128
	12	420.059	448.620	28.561	448.620	407.157	41.463	407.157	378.996	28.161

Observed sections		Channel width changing pattern								
		Channel Width 1990/m	Channel Width 2000/m	Diff.	Channel Width 2000/m	Channel Width 2010/m	Diff.	Channel Width 2010/m	Channel Width 2018/m	Diff.
Segment A		528.351	462.561	−65.79	462.561	546.444	83.883	546.444	260.065	−286.379
Segment B	1	445.321	390.687	−54.634	390.687	344.290	−46.397	344.290	295.775	−48.515
	2	482.050	604.926	122.876	604.926	506.433	−98.493	506.433	257.772	−248.661
	3	563.023	276.942	−286.081	276.942	375.623	98.681	375.623	251.507	−124.116
	4	416.867	361.382	−55.485	361.382	404.066	42.684	404.066	283.338	−120.728
	5	426.394	493.262	66.868	493.262	574.075	80.813	574.075	499.282	−74.793
	6	517.260	384.978	−132.282	384.978	373.713	−11.265	373.713	279.266	−94.447
	7	295.598	340.532	44.934	340.532	338.810	−1.722	338.810	301.933	−36.877
	8	403.172	382.629	−20.543	382.629	425.650	43.021	425.650	282.625	−143.025
	9	335.099	280.915	−54.184	280.915	375.704	94.789	375.704	271.114	−104.59
	10	353.189	395.769	42.58	395.769	461.849	66.08	461.849	481.140	19.291
	11	485.758	492.478	6.72	492.478	539.933	47.455	539.933	343.898	−196.035
	12	378.996	386.946	7.95	386.946	449.898	62.952	449.898	421.851	−28.047

channel migration occurred in section 12 accounting 1368 m and 1341 m respectively and migrated from the NE to NW direction (Fig. 8). During the 1990–2000 time interval, the analysis reveals that the maximum shift of the river channel (1910 m) was observed at section 3, whereas the lowest shifting (130 m) was detected at section 10, no shifting occurred in section 2 at all. Maximum right bank shifting (1042 m) observed in section 5, minimum was recorded (118 m) in section 11 whereas left bank showing 768 m (maximum) in section 6 and 21 m (minimum) in section 9 from 2000 to 2010. Within this time period, sections 1, 2 and 3 for both left and right bank moved NW. For all sections, shifting mainly occurred alternatively in NW and NE directions (Fig. 8).

In the recent decade, the shift of Gorai-Madhumati River is widespread in the leftward direction in almost all sections except 1 and 9. The highest shift was about 2906 m and 3009 m consecutively for right and left bank at section 7 and the lowest shifting at section 7 (47 m) for right bank and 42 m at section 9 for the left bank. The channel migration in both sides is very extensive due to decreasing in the river depth and water flow regime. It is clearly demonstrating that the abrasiveness of the river bank due to lithological weakness leads to an extensive

Table 3 Shifting along both banks of the river from 1972 to 2018. Here, RBS: Right Bank Shift, LBS: Left Bank Shift, DM: Direction of Migration

Observed sections		Channel shifting 1990 – 2000/m				Channel shifting 2000 – 2010/m				Channel shifting 2010 – 2018/m			
		RBS	DM	LBS	DM	RBS	DM	LBS	DM	RBS	DM	LBS	DM
Segment A		3261.96	358.48	3189.37	358.54	1067.78	181.34	989.95	181.39	1052.56	181.36	1265.13	181.40
Segment B	1	430.45	181.55	388.17	181.53	364.85	181.56	607.71	181.56	243.93	178.44	54.28	178.44
	2	0.00	0.00	298.83	207.69	230.08	161.56	247.14	105.52	583.023	356.74	734.10	335.51
	3	1910.44	88.40	1857.16	88.23	151.64	213.02	183.36	213.69	56.18	225.00	224.75	225.00
	4	712.34	51.34	640.66	23.38	317.85	53.13	572.45	88.09	1048.44	165.96	542.45	121.82
	5	551.60	242.54	458.99	210.82	1042.45	248.91	350.16	344.19	535.09	226.44	2115.28	243.97
	6	635.71	233.13	885.44	248.96	449.51	225.00	768.13	204.44	123.56	239.03	123.56	239.03
	7	170.84	150.25	229.20	123.69	521.21	243.43	767.84	230.59	2906.87	267.07	3009.04	269.59
	8	331.85	106.69	135.78	110.55	190.61	122.22	202.85	108.12	47.02	153.43	99.20	147.99
	9	220.01	50.19	111.35	55.30	37.3388	225.00	21.13	51.34	112.64	31.82	42.26	38.65
	10	130.46	225.00	100.23	212.47	342.86	227.72	96.32	208.61	54.36	225.00	70.87	229.39
	11	156.52	66.03	243.01	216.91	118.53	230.44	170.06	217.40	191.91	62.90	48.00	65.55
	12	251.67	340.14	355.61	33.69	172.96	351.25	65.75	0.871	218.97	318.65	326.65	319.89
Observed sections		**Channel shifting 1972 – 1977/m**				**Channel shifting 1977 – 1980/m**				**Channel shifting 1980 – 1990/m**			
		RBS	DM	LBS	DM	RBS	DM	LBS	DM	RBS	DM	LBS	DM
Segment A		3529.57	358.49	3364.63	358.47	1088.22	181.46	1117.08	181.52	2300.13	178.44	2036.51	178.45
Segment B	1	361.69	178.47	292.72	178.44	40.01	176.54	15.11	178.12	220.54	178.43	338.08	178.44
	2	200.19	277.59	152.27	92.48	65.14	293.96	606.41	333.43	847.21	222.78	1049.2	221.93
	3	687.12	185.97	437.26	199.09	223.36	157.39	90.60	217.87	647.86	222.64	701.76	222.79
	4	0.00	0.00	121.03	23.19	234.65	28.30	215.02	24.44	712.34	51.34	821.06	47.35
	5	305.70	278.97	121.03	113.19	56.85	116.56	60.30	108.43	432.47	114.30	160.06	173.15
	6	102.38	223.26	119.24	38.65	39.32	45.00	105.95	53.13	682.38	36.15	777.43	72.55
	7	569.38	135.00	534.82	146.30	114.11	291.80	255.16	94.76	494.24	149.03	570.56	164.93
	8	473.83	190.30	360.86	176.63	199.91	237.99	312,87	241.69	793.43	145.88	654.16	155.09
	9	148.06	92.72	116.10	79.38	194.78	40.60	174.93	40.10	303.80	45.93	319.32	48.57
	10	209.13	252.89	162.17	264.55	39.20	258.69	54.36	225.00	293.75	227.12	277.72	228.36
	11	357.88	69.44	1332.06	70.48	287.83	173.65	543.61	74.74	66.27	229.39	57.72	80.77
	12	716.82	268.94	538.12	296.87	332.94	9.09	118.53	273.17	1368.49	344.96	1341.49	0.84

rate of lateral migration. Shifting is very prominent in the downstream part especially in Segments A and B rather than the upstream region. This shifting is probably lithology and slope controlled. Anthropogenic causes like diversion for agriculture can also be claimed for the lateral migration in Segments A and B.

4.3 Sinuosity of the Gorai-Madhumati River

This investigation confirms that the sinuosity has changed throughout the study time span. In Segment A, calculated sinuosity was 6.38, 3.66, 4.18, 5.40, 3.19, 3.71, and 4.8 consecutively for the years of 1972, 1977, 1980, 1990, 2000, 2010, and 2018 (Table 4). On the other hand, segment B shows low sinuosity index throughout the respective years that was in and around 2 indicating meandering river. It is evident that the overall sinuosity has increased over time from 1977 to 1990. Overall sinuosity of the Gorai-Madhumati River is close to the average value of 1.80.

In the pre-barrage phase, topographic factors of flood plain (bank materials, valley alignment, number of bars, tectonic activity) along with monsoonal flood discharge and hydraulic factors, controlled sinuosity of the Gorai-Madhumoti River. After the installation of Farakka Barrage, hydraulic factors became the prime factor to control sinuosity. A drastic fall in discharge forced the channel to meander to dissipate less energy. The combined effect of sudden peak monsoonal discharge and flow controlling actions of Farakka Barrage authority results in a current increasing sinuous pattern. This implies erosion in one bank and deposition (point bars, scroll bars) in another one of meander bends. The construction of infrastructures (bridges, river ports, industries, and urban

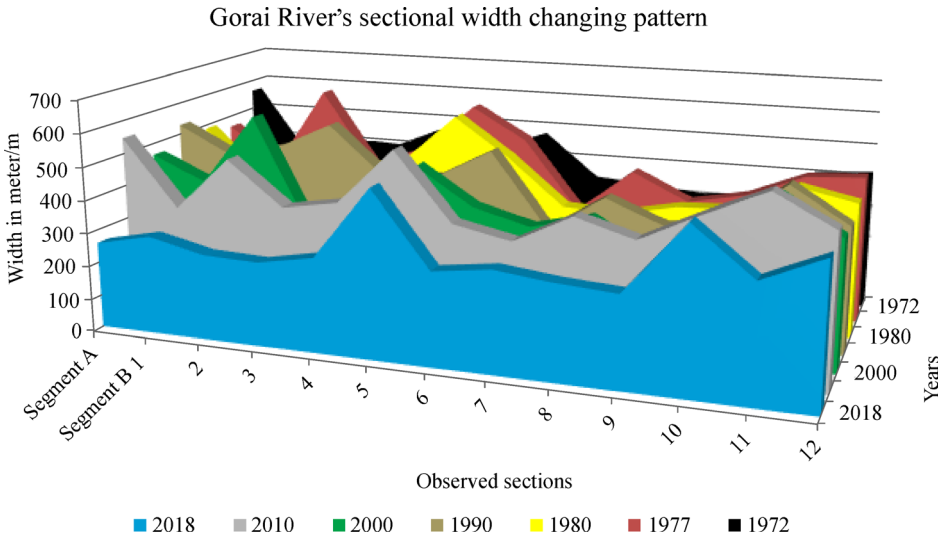

Fig. 6 The changes in the sections width in the different segments of Gorai-Madhumati River.

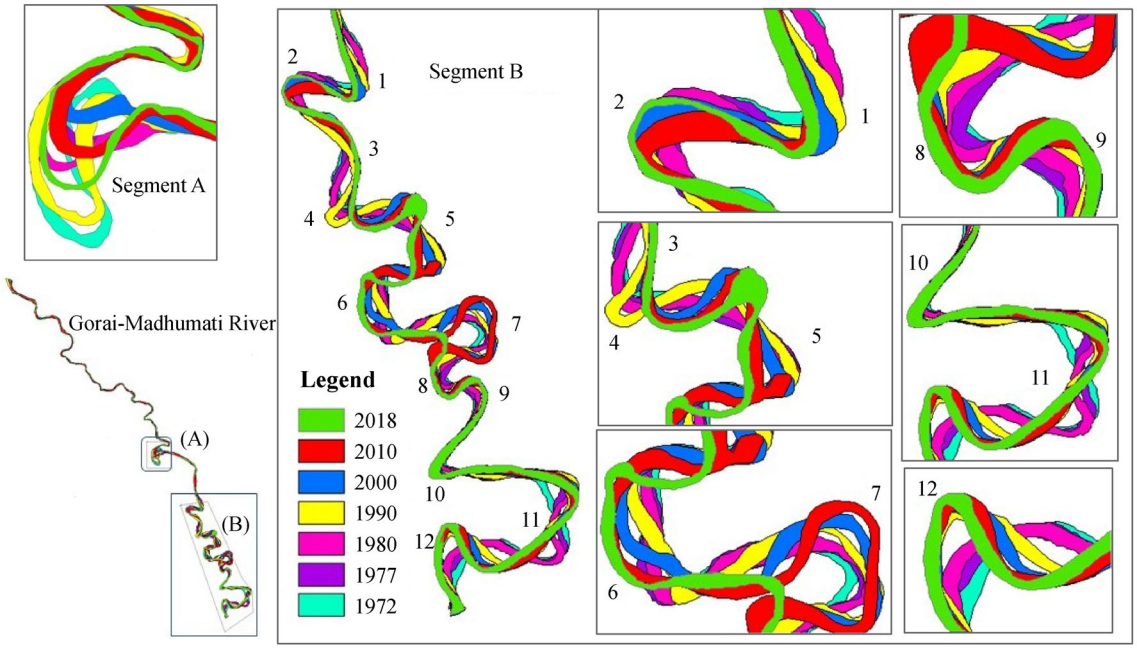

Fig. 7 Planform channel migration (shifting) of the Gorai-Madhumati River in the considered sections in seven different periods.

areas) along with river bank is very crucial to control and mange such erosive and depositing characteristics.

4.4 Erosion-accretion pattern on both sides of the river

Erosion and accretion have been observed from 1972 to 2018 similarly to the observed sections for shifting and river width. In Segment A, erosion was most pronounced from the period of 1980 to 1990, in contrast to other time spans. On the other hand, bank accretion was most prominent between 1990 and 2000. To summarize, net erosion and accretion in the Gorai-Madhumati reported as 17.38 and 15.49 km^2 respectively from 1972 to 1980 accounting about 1.89 km^2 land loss in that area (Fig. 9). Most extensive land loss figured out about 9.53 km^2 occurred in the following decades from 1980 to 1990. In the recent decade (2010–2018), huge landmass acquired approximately 12.94 km^2 representing 21.05 km^2 accreted land and concurrent 8.11 km^2 eroded landmass (Table 5). In addition, accretion was more dominant than erosion on both banks of the river from 1990 to 2000 exhibits 5.33 km^2 land gain. On the contrary, the 2000 to 2010 period inversely showing dominant erosional trend which signifies that about 15.62 km^2 landmass eroded and

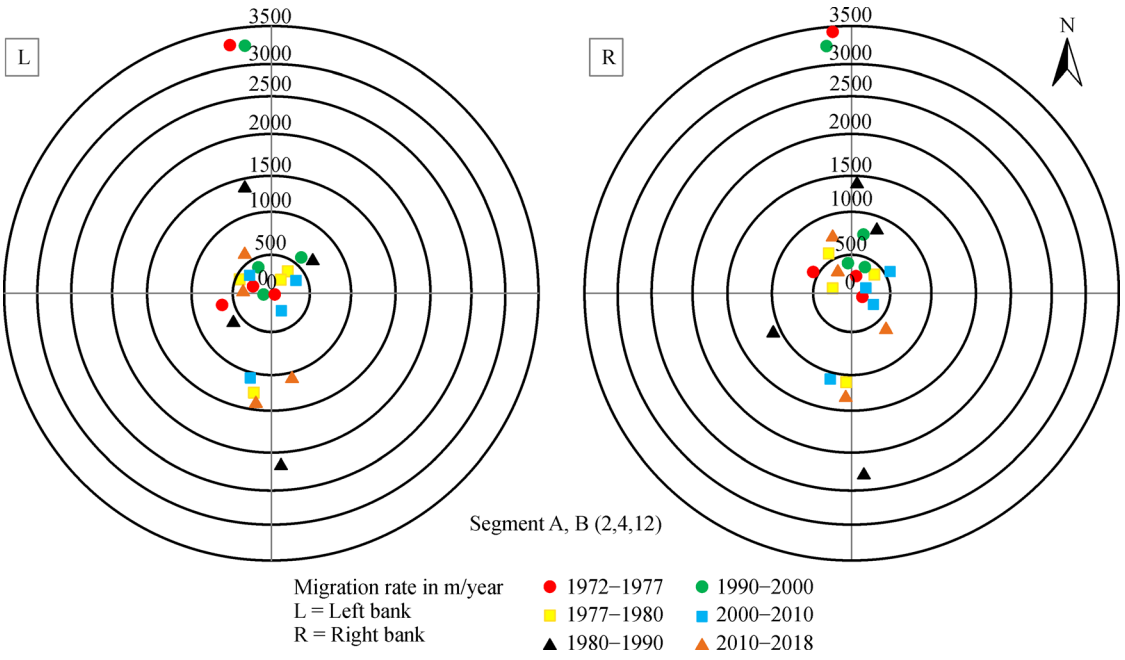

Fig. 8 Migration trend of the river bends in Segment A and Segment B (2, 4, and 12) throughout the study timeframe. Only the severe shifted bends are plotted in this diagram. Spatiotemporal migration direction denotes the vulnerable regions. Colored symbols in a specific time range showing migration trends of different segments in that periods (i.e., red circle showing migration distance and direction of mentioned segments from 1972 to 1977).

Table 4 Sinuosity in the segment A and B of the Gorai-Madhumati River

River reach	Sinuosity						
	1972	1977	1980	1990	2000	2010	2018
Segment A	6.38	3.66	4.18	5.40	3.19	3.71	4.8
Segment B	1.96	2.07	2.16	2.34	2.41	2.45	2.24
Overall	1.78	1.70	1.79	1.88	1.85	1.87	1.87

concurrent 11.13 km^2 area accreted in that respective time domain (Fig. 9). Throughout the 50 years of the study period, the total river bank erosion was lower than the amount of accretion representing 80.84 and 82.9 km^2 consecutively (Fig. 10). However, natural factors, i.e., water discharge, velocity, sediment volume, and climate etc. are responsible for the fluctuation of erosion-accretion in the river.

4.5 Sand bar morphodynamics within the river channel

Morphodynamics of the sand bars documented in this research mainly in the three locations where the bars developed and most change occurred within the river channel identified as sandbar-I (in Segment A), II and II (in Segment B). Actually, the Gorai-Madhumati River channel is choked by the sandbars in this selected section and this channel generally fades during winter and becomes activated during flood season by water flow. The study has found that sandbar-I progressively expanded from 1972 to 1980 then declined up to 2000; afterwards, the bar area expanded until 2018. Total aerial expansion in sandbar-I was about 1.475 km^2 from 1972 to 2018 (Table 6). The shape of the sandbar altered from lens to arcuate shape with the modification of channel configuration (Fig. 11). However, it is apparently showing that sandbar-II squeezed from 1.148 to 0.967 km^2 between 1972 and 1990. But the area increased dramatically in the following decades up to 2.014 km^2 in 2018. The shape of sandbar-II remains unchanged except for the addition and removal of landmasses due to the fluctuation of sediment supply and river discharge (Fig. 11). The data analysis reveals that the area in sandbar-III has increased significantly throughout the study period from 0.444 to 1.751 km^2. It can be concluded that overall area in the three sandbars increased significantly to 2010 to 2018. Sand bar area can be clearly correlated with the net gain and loss in a respective time frame. It is evident that net land gain is maximum between 2010 and 2018 accounting for 21.05 km^2 land accretion. This accretion has also been reflected in the three-sand bar area, representing aerial growth.

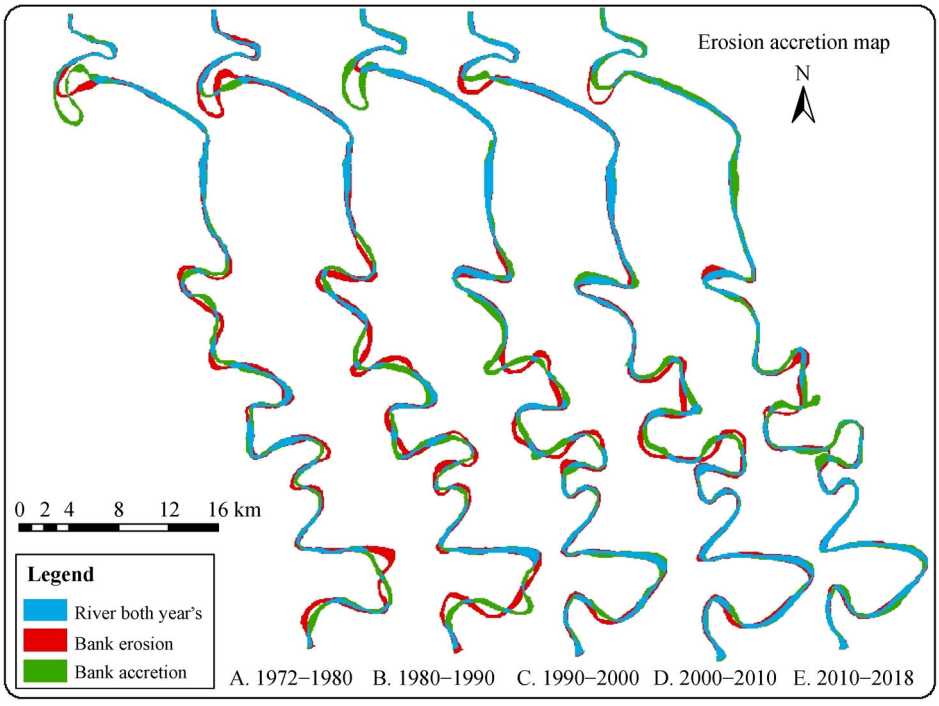

Fig. 9 The net erosion (the red color) and the net accretion (the green color) in five consecutive time spans in the study area, where the blue color demonstrates the unchanged channel within each time spans. The area between the green and the red color has experienced erosion, at first. Thereafter, accretion has occurred in the same area. Consequently, net change was zero and this area has been left colorless.

Table 5 Net erosion-accretion and gain-loss from 1972 to 2018 in the Gorai-Madhumati River

Time period	Net erosion/km^2	Net accretion/km^2	Net land gain (+) or loss (-)
1972–1980	17.38	15.49	−1.89
1980–1990	25.3	15.77	−9.53
1990–2000	14.13	19.46	+ 5.33
2000–2010	15.62	11.13	−4.49
2010–2018	8.11	21.05	+ 12.94

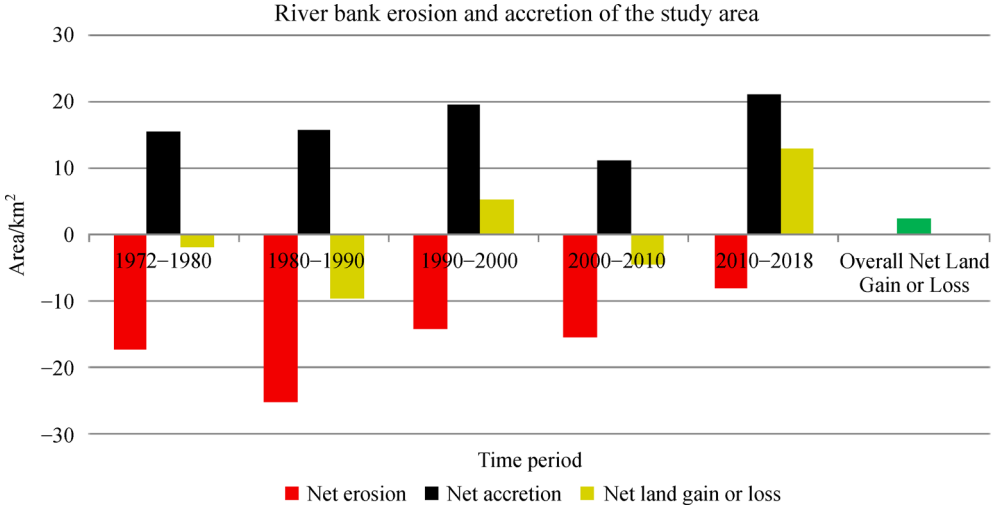

Fig. 10 River bank erosion-accretion and the total gain-loss (1972–2018) of the study area.

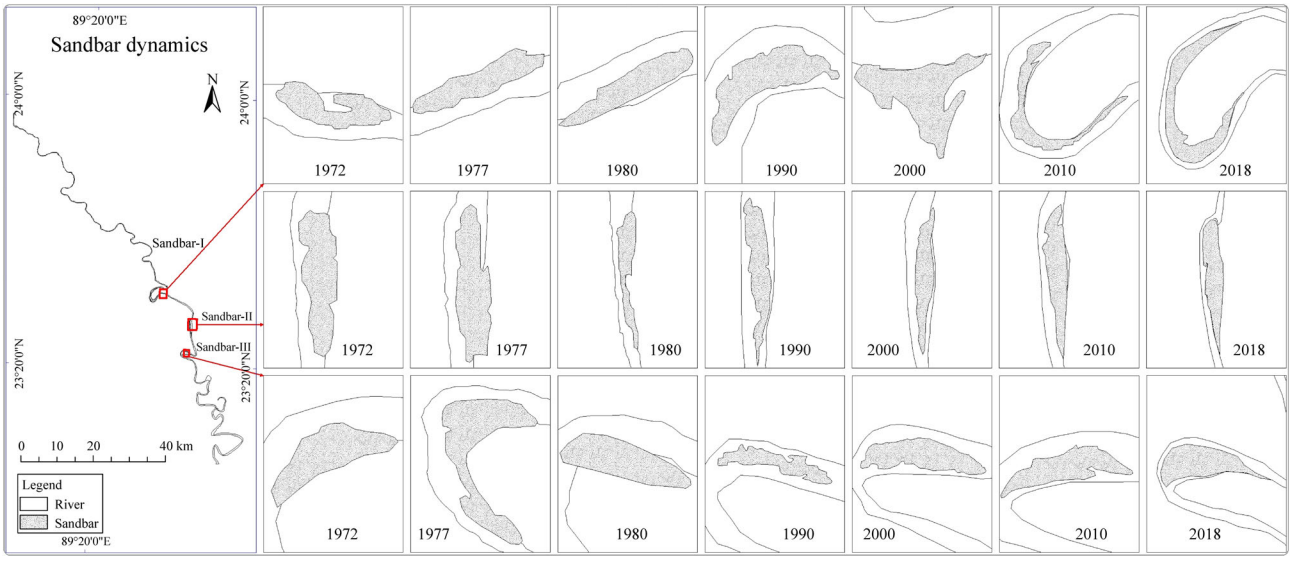

Fig. 11 Spatio-temporal distribution of sandbars in the active river channel of the Gorai-Madhumati River in seven different time period.

Table 6 Aerial statistics of sandbars (Charland) of the Gorai-Madhumati River 1972–2018

Area	1972	1977	1980	1990	2000	2010	2018
Sandbar-I	0.531	0.592	0.598	0.471	0.354	0.797	2.006
Sandbar-II	1.148	1.069	1.018	0.967	1.152	1.628	2.014
Sandbar-III	0.444	1.496	0.41	0.445	1.078	0.526	1.751

4.6 Impacts of Farakka Barrage in the river migration and dynamics

Farakka Barrage was constructed on 21 April, 1975 in the main stem of Ganges River to divert and supply fresh water to Kolkata city. Analysis on the historical discharge data from 1960 to 2010 at Hardinge Bridge station in Bangladesh revealed that remarkable drop down in the water flow of Gorai-Madhumati River and downstream distributaries of the Ganges River occurred post Farakka

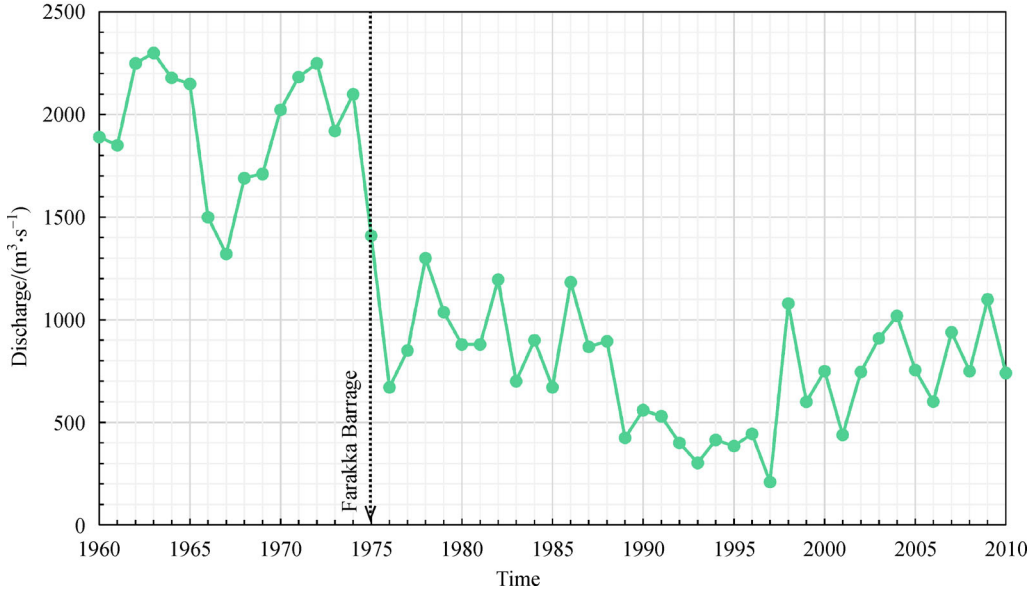

Fig. 12 Discharge with time near Hardinge Bridge from 1960 to 2010. Dotted line indicating the discharge drop due to the construction of Farakka Barrage in 1975 at the upstream part near India.

periods (1975–2019) (Fig. 12). Not only the impediments in hydrological flows but significant changes also happened in river sectional width, sand bar morphodynamics, shifting trend, and erosion-accretion history due to Farakka Barrage. In comparison to pre and post Farakka period from 1972 to 1977, river width significantly increased from 404 to 603 m in section 2 and section 5 witnessed about 174 m width increase in this time frame due to recession in flow and subsequent siltation in river bed. There is a gradual increase in the aerial extent of the observed sandbars from 1972 to 2018. From 1972 to 2018, sandbar-I, II, III show about 1.47, 0.87, and 1.30 km^2 consecutive spatial expansion on settling huge amount sediments. Remarkable amounts of accretion and continuous land gain was also noticed after the Farakka Barrage project from 1972 to present. Throughout the study period, about 5.56 km^2 land accreted on the both banks of Gorai-Madhumati River. Owing to significant dropping of water flow at Farakka for nearly 40 years, regions adjacent to the Gorai-Madhumati river basin have been suffering from environmental degradation.

5 Conclusions

The present study intends to comprehend the spatiotemporal changes in the channel width, shifting, sinuosity, erosion-accretion, and channel bar morphodynamics along with the impacts of Farakka Barrage on the observed parameters and factors. For this purpose, we have utilized Landsat satellite images from 1972 to 2018. The spatiotemporal investigation specifies that channel shifting was most prominent in segment A. In the recent time (2010–2018), Gorai-Madhumati River shifting expansion was widespread in the leftward course in all sections except sections 1 and 9. The attained outcomes also indicate that the narrowest width of the channel observed in segment A and section 3 in segment B from 2010 to 2018 indicate a significant depositional phase due to river bed siltation. In contrast, the highest width was observed in section 2 in segment B from 1972 to 1977 indicating a significant erosional event. Furthermore, sandbars became enlarged significantly and got their aerial extent by depositing sediments within the river channel, especially from 2010 to 2018. To be more precise, the 1972 to 1980 and 2000 to 2010 time spans were reported as a loss period, although most extensive land loss occurred from 1980 to 1990. On the other hand, there were huge landmass gains of almost 12.94 km^2 from 2010 to 2018. Moreover, Farakka Barrage played a negative role in planform mobility, discharge, erosion-accretion, and siltation of the river from 1977 to 2018. Throughout the study period, it is evident that the Gorai-Madhumati River has been experiencing extreme siltation which subsequently causes numerous problems in the river basin areas. This siltation event can be clearly correlated with drastic reduction in water discharge due to the construction of Farakka Barrage.

Acknowledgements Authors really appreciate to Dr. Anwar Zahid, Deputy Director, BWDB, for proving available data to conduct the study. We are pleased to acknowledge the department of Geology, University of Dhaka for giving us the laboratory amenities to perform software analysis. The authors are also thankful to the anonymous reviewers for their comments and suggestions.

References

Adams W C (1919). History of the Rivers in the Genetic delta, 1750–1918. East Pakistan: Bengal Secretariat Press

Ahmed S J, Islam S (2003). Banglapedia: National Encyclopedia of Bangladesh (Available at Banglapedia website)

Bag R, Mondal I, Bandyopadhyay J (2019). Assessing the oscillation of channel geometry and meander migration cardinality of Bhagirathi River, West Bengal, India. J Geogr Sci, 29(4): 613–634

Bangladesh Bureau of Statistics (BBS) (2016). Statistical Year Book of Bangladesh. Dhaka

Bhuiyan M A, Kumamoto T, Suzuki S (2015). Application of remote sensing and GIS for evaluation of the recent morphological characteristics of the lower Brahmaputra-Jamuna River, Bangladesh. Earth Sci Inform, 8(3): 551–568

Biswas N B, Ahammad B M (2014). Application of CCHE2D mathematical model in the Gorai Offtake for two-dimensional simulation. International Journal of Surface and Groundwater Management, 1(1): 52–58

Clijncke A (2001). Morphological response to dredging of the upper Gorai River. Dissertation for Master Degree. Delft: TU Delft

Dabojani D, Mithun D, Kanak Kanti K (2014). River Change Detection and Bankline Erosion Recognition using Remote Sensing and GIS. Forum Geografic, XIII(1):12–17

Das A K, Sah R K, Hazarika N (2012). Bankline change and the facets of riverine hazards in the floodplain of Subansiri–Ranganadi Doab, Brahmaputra Valley, India. Nat Hazards, 64(2): 1015–1028

DHI (Delft Hydraulic Institute) (1996). River survey project (FAP 24)–morphology of Gorai off-take: special report No.10. Dhaka: WARPO

Downward S R, Gurnell A M, Brookes A (1994). A methodology for quantifying river channel planform change using GIS. IAHS Publications-Series of Proceedings and Reports-Intern Assoc Hydrological Sciences, 224: 449–456

EGIS (Environmental and Geographical Information System) (2000). Environmental baseline of Gorai river restoration project, EGIS-II. Dhaka: Ministry of Water Resources

Fuller I C, Large A R G, Milan D J (2003). Quantifying channel development and sediment transfer following chute cutoff in a wandering gravel-bed river. Geomorphology, 54(3–4): 307–323

Ghoshal S, James A L, Singer M B, Aalto R (2010). Channel and floodplain change analysis over a 100-year period: lower Yuba River, California. Remote Sens, 2(7): 1797–1825

Gurnell A M (1997). Channel change on the River Dee meanders, 1946–1992, from the analysis of air photographs. Regulated Rivers: Research & Management, 13(1): 13–26

Halcrow and Partners Ltd., DHI, EPC Ltd., Sthapati Sangshad Ltd. (FAP

4) (1993). Morphological studies: southwest area water resources management project. In: Report Produced for Flood Plan Coordination Organization (FPCO). Dhaka: Bangladesh

Hasan M I, Rahman M M, Ahsan M, Haque M (2015). Meandering bend development process in Gorai-Madhumati River. In: 5th International Conference on Water & Flood Management (ICWFM-2015)

Hore S K, Sarker M H, Ferdous M R, Ahsan M, Hasan M I (2013). Study of the off-take dynamics for restoring the Gorai River. In: 4th International Conference on Water & Flood Management. Dhaka

Islam G T, Karim M R (2005). Predicting downstream hydraulic geometry of the Gorai River. Journal of Civil Engineering, 33(2): 55–63 (IEB)

Islam M S, Sultana S, Saifunnahar M, Miah M A (2014). Adaptation of char livelihood in flood and river erosion areas through indigenous practice: a study on Bhuapur riverine area in Tangail. J Environ Sci Nat Resour, 7(1): 13–19

Islam S (2003). Banglapedia: National Encyclopedia of Bangladesh. Dhaka: Asiatic society of Bangladesh

Islam S N (2016). Deltaic floodplains development and wetland ecosystems management in the Ganges–Brahmaputra–Meghna Rivers Delta in Bangladesh. Sustainable Water Resources Management, 2(3): 237–256

Islam S N, Gnauck A (2011). Water shortage in the Gorai River Basin and damage of mangrove wetland ecosystems in Sundarbans, Bangladesh. In: 3rd International Conference on Water & Food Management (ICWFM-2011). Dhaka

Khanam M, Navera U K (2016) Hydrodynamic and morphological analysis of Gorai River using delft 3d mathematical model. In: Proceedings of the 3rd International Conference on Civil Engineering for Sustainable Development (ICCESD). Khulna

Kummu M, Lu X X, Rasphone A, Sarkkula J, Koponen J (2008). Riverbank changes along the Mekong River: remote sensing detection in the Vientiane-Nong Khai area. Quat Int, 186(1): 100–112

Langat P K, Kumar L, Koech R (2019). Monitoring river channel dynamics using remote sensing and GIS techniques. Geomorphology, 325: 92–102

Li L, Lu X X, Chen Z (2007). River channel change during the last 50 years in the middle Yangtze River, the Jianli reach. Geomorphology, 85(3–4): 185–196

Magliulo P, Bozzi F, Pignone M (2016). Assessing the planform changes of the Tammaro River (southern Italy) from 1870 to 1955 using a GIS-aided historical map analysis. Environ Earth Sci, 75(4): 355

Marston R A, Girel J, Pautou G, Piegay H, Bravard J P, Arneson C (1995). Channel metamorphosis, floodplain disturbance, and vegetation development: Ain River, France. Geomorphology, 13(1–4): 121–131

McFeeters S K (1996). The use of the Normalized Difference Water Index (*NDWI*) in the delineation of open water features. Int J Remote Sens, 17(7): 1425–1432

Mondal I, Thakur S, Bandyopadhyay J (2020). Delineating lateral channel migration and risk zones of Ichamati River, West Bengal, India. J Clean Prod, 244: 118740

Morisawa M. (1985). Rivers: form and process. Geomorphology texts, (7)

Rinaldi M (2003). Recent channel adjustments in alluvial rivers of Tuscany, Central Italy. Earth Surf Process Landf, 28(6): 587–608

Surian N (1999). Channel changes due to river regulation: the case of Piave River, Italy. Earth Surf Process Landf, 24(12): 1135–1151

Surian N, Rinaldi M (2003). Morphological response to river engineering and management in alluvial channels in Italy. Geomorphology, 50(4): 307–326

Winterbottom S J (2000). Medium and short-term channel planform changes on the Rivers Tay and Tummel, Scotland. Geomorphology, 34(3–4): 195–208

Xu H (2006). Modification of normalised difference water index (*NDWI*) to enhance open water features in remotely sensed imagery. Int J Remote Sens, 27(14): 3025–3033

Yang S L, Zhao Q Y, Belkin I M (2002). Temporal variation in the sediment load of the Yangtze River and the influences of human activities. J Hydrol (Amst), 263(1–4): 56–71

Yang C, Cai X, Wang X, Yan R, Zhang T, Zhang Q, Lu X (2015). Remotely sensed trajectory analysis of channel migration in Lower Jingjiang Reach during the period of 1983–2013. Remote Sens, 7 (12): 16241–16256